

LATE-TYPE FIELD STARS IN THE RASS AT HIGH GALACTIC LATITUDE

F.-J. Zickgraf¹, J. Krautter², S. Frink³, J.M. Alcalá⁴, R. Mujica⁵, E. Covino⁴, and M.F. Sterzik⁶

¹Hamburger Sternwarte, Gojenbergsweg 112, 21029 Hamburg, Germany

²Landessternwarte Königstuhl, D-69117 Heidelberg, Germany

³Sterrewacht Leiden, P.O. Box 9513, NL-2300 RA Leiden, The Netherlands

⁴Osservatorio Astronomico di Capodimonte, Via Moiariello 16, I-80131 Napoli, Italy

⁵Instituto Nacional de Astrofisica, Optica y Electronica, A. Postal 51 y 216 Z.P., 72000 Puebla, Mexico

⁶European Southern Observatory, Alonso de Cordova 3107, Santiago 19, Chile

ABSTRACT

We present results of an investigation on a high-galactic latitude sample of late-type field stars selected from the ROSAT All-Sky Survey (RASS). The sample comprises ~ 200 G, K, and M stars. Lithium abundances were determined for ~ 180 G-M stars. Radial velocities were measured for most of the ~ 140 G and K type stars. Combined with proper motions these data were used to study the age distribution and the kinematical properties of the sample. Based on the lithium abundances half of the G-K stars were found to be younger than the Hyades (660 Myr). About 30% are comparable in age to the Pleiades (100 Myr). A small subsample of 10 stars is younger than the Pleiades (100 Myr). They are therefore most likely pre-main sequence stars. Kinematically the PMS and Pleiades-type stars appear to form a group with space velocities close to the Castor moving group but clearly distinct from the Local Association.

Key words: Surveys – X-rays: stars – Stars: late-type – Stars: pre-main sequence

1. INTRODUCTION

In a previous investigation a sample of RASS X-ray sources located at $|b| \geq 20^\circ$ and $DEC \geq -9^\circ$ has been identified optically (Zickgraf et al. 1997). The sample comprises 674 X-ray sources distributed in 6 study areas with a total area of 685 deg² (see Fig. 1). The sample contains 273 stellar X-ray emitters of spectral type F to M plus 20 other stellar sources (CVs, WDs, A stars). The rest are extragalactic X-ray emitters and a few unidentified sources. The catalogue of identifications and the statistical analysis can be found in Appenzeller et al. (1998) and Krautter et al. (1999), respectively. Here we present the results of an investigation of the X-ray properties, the age distribution and the kinematics of the stellar subsample of coronal emitters.

2. OBSERVATIONS

The stellar counterparts of spectral types G to M were observed spectroscopically in the red wavelength region

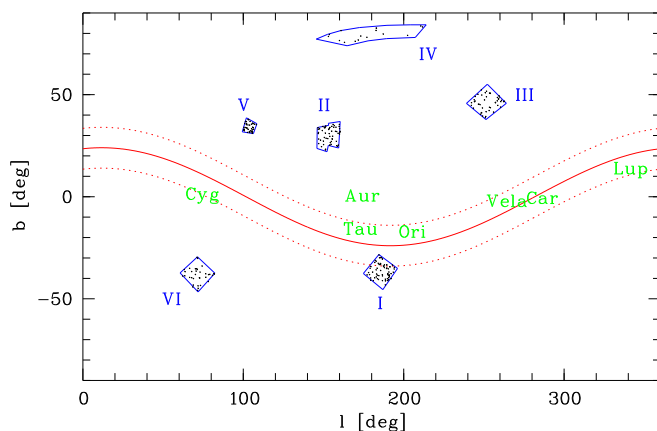


Figure 1. Location of the 6 study areas in galactic coordinates. Also shown is the Gould Belt according to Guillout et al. (1998).

containing the line $\text{Li I } \lambda 6708 \text{ \AA}$ during several observing campaigns between 1996 and 2002 mainly at Calar Alto Observatory. Further observations were obtained at Obs. Haute Provence and at ESO, La Silla. F stars were omitted because the Li I line is not a sensitive age indicator for these stars. We observed 172 of 199 stars with spectral types G to M. Data for 6 further G-K stars were found in the literature. Of the 141 G and K stars 118 were sufficiently bright ($V \leq 12^m$) for high-resolution spectroscopy with a resolution of $\Delta\lambda \sim 0.2 - 0.3 \text{ \AA}$ at 6708 \AA . Likewise, 7 M stars could be observed with high resolution. Fainter stars were observed with low spectral resolution of $\Delta\lambda \sim 3-4 \text{ \AA}$. Seven 7 G-K stars and 13 M stars are still unobserved. In total, spectroscopic observations of 179 out of 199 G, K, and M stars are available.

Radial velocities (RVs) and projected rotational velocities, $v \sin i$, were derived from the high-resolution spectra by means of cross-correlation techniques.

3. RESULTS

3.1. DISTANCES

The distances towards the G and K stars were derived from trigonometric or spectroscopic parallaxes. The high-resolution spectra allowed the determination of the luminosity classes and hence of the absolute visual mag-

nitudes, M_V . For the classification procedure spectra of MK standard stars were taken from the stellar library of Prugniel & Soubiran (2001). In this way spectroscopic parallaxes could be derived for 75 G-K stars. For M stars we obtained IR photometric parallaxes. 43 stars have IR photometry in the 2MASS catalogue. In the (J-H)-(H-K) diagram the M stars are located along the track for main-sequence stars. Distances were therefore derived for M_V magnitudes of main-sequence stars. Distances for 26 G-K stars and 4 M stars were found in the Hipparcos catalogue. For further 7 M stars trigonometric parallaxes were found in Gliese & Jahreiss (1991). In total, distances could be determined for 101 G-K and 54 M stars. For the remaining stars we assumed luminosity class V for the estimation of a lower limit for the distance.

The distribution of distances shows a maximum around 50 pc and a tail extending up to several 100 pc with most stars being nearer than 300 pc.

3.2. X-RAY LUMINOSITIES

Using these distances X-ray luminosities $L_X(0.1-2.4\text{keV})$ and bolometric luminosities L_{bol} were calculated. The ratio L_X/L_{bol} is shown in Fig. 2 as a function of bolometric magnitude, M_{bol} . The highest ratio is measured for the latest spectral types which have the faintest M_{bol} .

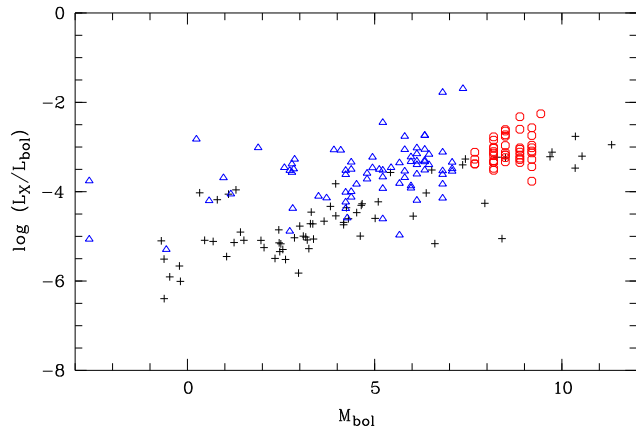


Figure 2. Ratio of X-ray and bolometric luminosity for all single stars with trigonometric (+ sign), spectroscopic (triangles), or IR photometric parallaxes (circles) as a function of bolometric magnitude, M_{bol} .

3.3. LITHIUM ABUNDANCES

Equivalent widths of $\text{Li I } \lambda 6708$, $W(\text{Li})$, were measured in high resolution spectra by direct integration. The contribution of $\text{Fe I } \lambda 6708.44\text{\AA}$ was taken into account. The detection limit was $\sim 10\text{m\AA}$. In low/medium resolution spectra $\text{Li I } \lambda 6708$ is blended with $\text{Fe I } \lambda 6703$, 6705 , and 6710\AA . The contributions of the individual lines were sep-

arated by means of the fitting method described by Zickgraf et al. (1998). The detection limit in the low/medium resolution spectra is $\sim 60\text{m\AA}$ for K stars and $\sim 200\text{m\AA}$ for M stars. The equivalent widths are displayed in Fig. 3 as function of effective temperature, T_{eff} . Conversion of $W(\text{Li})$ to abundances $N(\text{Li})$ was performed using the curves of growth of Soderblom et al. (1993) for $T_{\text{eff}} \geq 4000\text{K}$ and Pavlenko & Magazzù (1996) for cooler stars. We applied the spectral type - T_{eff} relations of de Jager & Nieuwenhuijzen (1987). The estimated temperature uncertainty is $\sim 200\text{K}$ which leads to an average error of $N(\text{Li})$ of $\approx 0.3\text{dex}$. In Fig. 4 $N(\text{Li})$ is displayed as function of T_{eff} . Included in the figure are the upper and lower envelope of $N(\text{Li})$ for the Pleiades, upper envelopes for the Ursa Major Moving Group (UMaG) and for the Hyades, respectively.

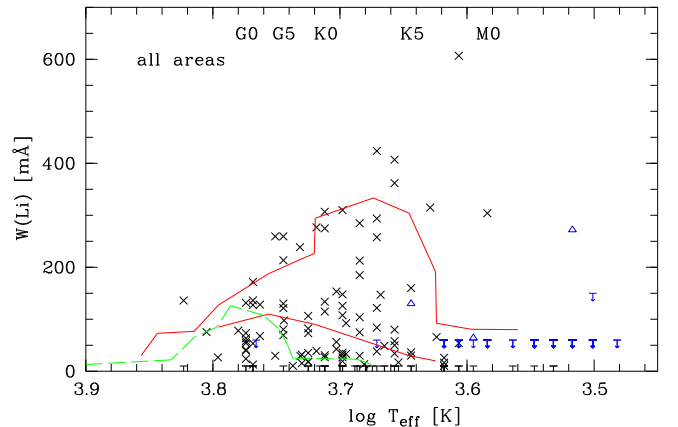


Figure 3. Equivalent widths of $\text{Li I } \lambda 6708$ as a function of T_{eff} for all stars in the six study areas. Crosses and triangles are high and low resolution measurements, respectively. The solid lines denote the upper and lower envelope of the lithium equivalent widths in the Pleiades adopted from Soderblom et al. (1993). The dashed line shows the upper envelope for the Hyades cluster taken from Thorburn et al. (1993).

3.4. AGE ESTIMATES

Age groups were defined based on lithium abundances, $N(\text{Li})$, and on the comparison with the $N(\text{Li})$ distribution in the Pleiades (100 Myr), UMaG (300 Myr) and Hyades (660 Myr). The age group PMS contains stars with $N(\text{Li})$ above the Pleiades upper envelope, and the age group PL_ZAMS comprises stars with $N(\text{Li})$ between the Pleiades upper and lower envelope. The age group UMa consists of stars between the Pleiades lower envelope and Hyades upper envelope, and age group Hya+ has $N(\text{Li})$ below the Hyades upper envelope. The assigned ages and fractions of G-K stars in each age group are summarized in Table

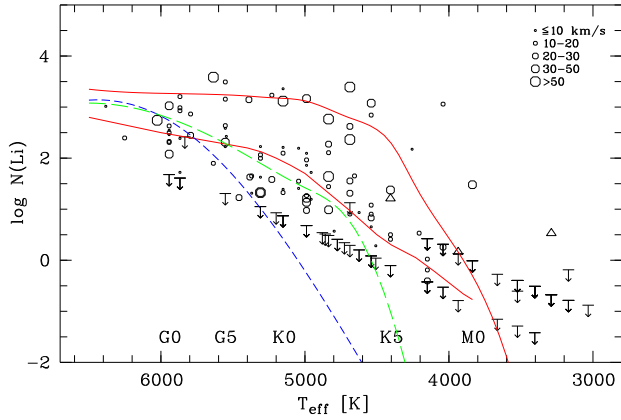


Figure 4. Lithium abundances versus effective temperature for the complete sample. Upper limits are plotted as downward arrows. Circles denote high-resolution measurements with the symbol size depending on $v \sin i$. Low and medium resolution data are plotted as triangles. The solid lines are the upper and lower limit of $\log N(\text{LiI})$ in the Pleiades; the long dashed and short dashed lines show the upper $\log N(\text{LiI})$ limits for the UMaG and the Hyades, respectively.

Table 1. Statistics of the age distribution of the sample of G-K stars. The total number of G-K stars is 141. The third line gives the median rotational velocity in km s^{-1} .

	age group			
	PMS < 100 Myr	PL_ZAMS 100 Myr	UMa ~ 300 Myr	Hya+ > 660 Myr
number	8	40	19	74
fraction	6%	28%	13%	52%
$\langle v \sin i \rangle_{\text{med}}$	32	17	18	11

1 together with the median rotational velocity, $v \sin i$ of the respective age group. Obviously, $v \sin i$ decreases with increasing age.

3.5. AGE DEPENDENT $\log N - \log S$ DISTRIBUTION

We compared the observed cumulative number distribution, $\log N(> S) - \log S$, of our sample with model predictions by Guillout et al. (1996). The models give cumulative surface densities, $N(> S)$, as a function of ROSAT-PSPC count rate, S , for three age bins: age younger than 150 Myr, age between 150 Myr and 1 Gyr, and older than 1 Gyr. We restricted the comparison to the youngest model age bin and to the sum of all model age bins because of the difficulty to separate observationally stars with ages of several 100 Myr to ~ 1 Gyr and older. In Fig. 5 the comparison is shown for the stars in the five study areas located around $|b| = 30^\circ$. Shown are the sum of all age groups and of the sum of age groups PMS, PL_ZAMS, and of PMS, PL_ZAMS, and UMa which represent the

subsample younger than about 150 Myr. The comparison shows that the observed numbers of stars are in reasonably good agreement with the model predictions. This holds for both the sum of all age groups and stars younger than ~ 150 Myr obtained as described above and represented in the figure by the filled symbols. Likewise, the predicted flattening of $\log N(> S) - \log S$ at increasing smaller count rates is also found in our data for area V which has the lowest count rate limit of 0.01 cts s^{-1} .

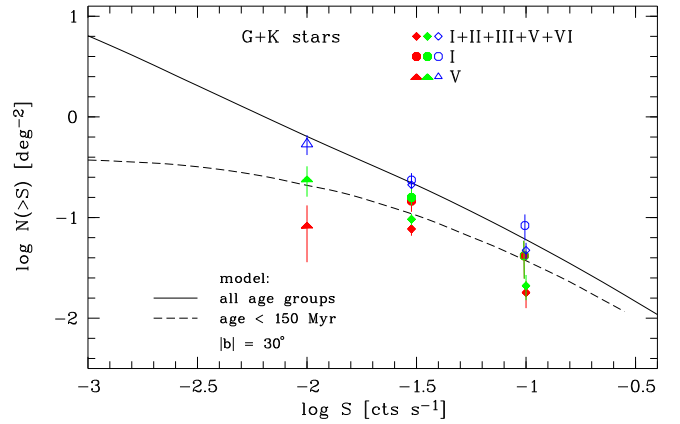


Figure 5. Comparison of observed coadded number densities of G and K stars, $N(> S)$, for three RASS count rates S with models of Guillout et al. (1996) for $|b| = 30^\circ$. Open symbols denote the sum of all age groups. Lower and upper filled symbols represent the sum of age groups PMS and PL_ZAMS, and of PMS, PL_ZAMS, and UMa, respectively.

3.6. KINEMATICS

Proper motions were obtained for 138 G, K, and M stars from the Hipparcos, TYCHO-2, UCAC2, and STARTNET catalogues. Space velocity components U , V , and W were calculated in the Local Standard of Rest (LSR) (right-handed coordinate system) for 89 single G-K and 8 M stars with distance, RV, and proper motion. For the correction of the solar motion we used the solar motion vector of Dehnen & Binney (1998).

For the youngest age groups PMS and PL_ZAMS an $U - V$ digram is shown in the upper panel of Fig. 6. The space velocities U and V of these stars cluster with a few exceptions around two values. The majority is found close to the velocity of the Castor Moving Group (MG). A second but much smaller fraction is located close to the Local Association (“local” in Fig. 6). The figure also shows that most PMS stars are kinematically consistent with the Castor MG but distinct from the Local Association.

This finding is also consistent with the velocity component in the direction perpendicular to the galactic plane, W , which is shown in the $W - V$ diagram in the lower

panel of Fig. 6. As for U and V most PMS stars are kinematically distinct from the Local Association also in the W space velocity component.

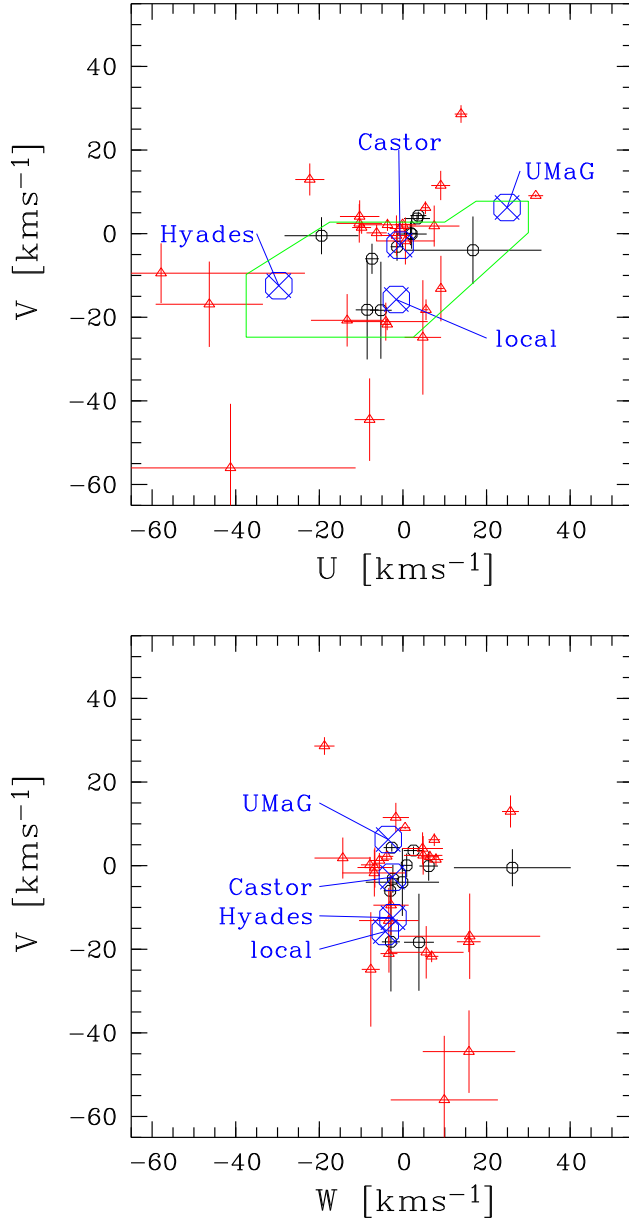


Figure 6. Upper Panel: $U - V$ diagram for PMS (\circ) and PL-ZAMS stars (\triangle). Included are the limits for young disk stars from Eggen (1989) and space velocities of the indicated clusters and MGs from Montes et al. (2001). Lower panel: $W - V$ diagram for the same sample of stars. Velocities are in the LSR reference frame.

4. CONCLUSIONS

For the age distribution of the high-galactic latitude coronal sample we found that about half of the G-K stars are younger than the Hyades. About 1/3 of the G-K stars is as young or younger than the Pleiades. A small fraction of less than 10% of the G-K stars is younger than the Pleiades. In contrast to the PLZAMS group whose members are found in all study areas most PMS stars, i.e. 8 out of 10, are located in area I. Only two PMS stars are found in area II and none in the remaining areas. This could indicate a possible relation of the high $|b|$ PMS stars to the Gould Belt indicated in Fig. 1. However, the subsample formed by combining the stellar age groups PMS and PLZAMS is spatially distributed in all directions covered by our study areas. At the same time most of its members show similar kinematical parameters independent of spatial location. This questions the relation to the Gould Belt. Rather, the space velocities are consistent with these stars being members of a loose moving group with velocities close to the Castor MG which has an age of $\sim 200 \pm 100$ Myr (Barrado y Navascués 1998). If the members of the PMS group of our sample belong indeed to Castor MG this would indicate an even larger spread of age in this moving group.

REFERENCES

- Appenzeller, I., Thiering, I., Zickgraf, F.-J. et al., 1998, ApJS 117, 319
 Barrado y Navascués, D. 1998, A&A 339, 831
 Dehnen W., Binney, J.J., MNRAS 298, 387
 de Jager, C. & Nieuwenhuijzen, H. 1987, A&A 177, 217
 Eggen, O.J., 1989, PASP 101, 366
 Gliese, W. & Jahreiss, H. 1991, Nearby Stars, Preliminary 3rd Version, Astron. Rechen-Institut, Heidelberg
 Guillout, P., Haywood, M., Motch, C. & Robin, A.C 1996, A&A 316, 89
 Guillout, P., Sterzik, M.F, Schmitt, J.H.M.M., et al. 1998, A&A 334, 540
 Krautter, J., Zickgraf, F.-J., Thiering, I., et al. 1999, A&A 350, 743
 Montes, D., López-Santiago, J., Gálvez, M.C., et al. 2001, MNRAS 328, 45
 Pavlenko, Y.V. & Magazzù, A. 1996, A&A 311, 961
 Prugniel, Ph. & Soubiran, C., 2001, A&A 369, 1048
 Soderblom, D.R., Jones, B.F., Balachandran, S., et al. 1993, AJ 106 1059
 Thorburn, J.A., Hobbs, L.M., Deliyannis, C.P., & Pinsonneault, M.H. 1993, ApJ 415, 150
 Zickgraf, F.-J., Thiering, I., Krautter, J. et al. 1997, A&AS 123, 103
 Zickgraf, F.-J., Alcalá, J.M., Krautter, J. et al., 1998, A&A 339, 457